Dilation of the giant vortex state in a mesoscopic superconducting loop

S. Pedersen,* G. R. Kofod, J. C. Hollingbery, C. B. Sørensen, and P. E. Lindelof
The Niels Bohr Institute, University of Copenhagen, Universitetsparken 5, DK-2100 Copenhagen, Denmark
(Received 1 April 2001; published 23 August 2001)

We have experimentally investigated the magnetization of a mesoscopic aluminum loop at temperatures well below the superconducting transition temperature T_c. The flux quantization of the superconducting loop was investigated with a μ-Hall magnetometer in magnetic field intensities between ± 100 G. The magnetic field intensity periodicity observed in the magnetization measurements is expected to take integer values of the superconducting flux quanta $\Phi_0 = h/2e$. A closer inspection of the periodicity, however, reveals a subflux quantum shift. This fine structure we interpret as a consequence of a so-called giant vortex state nucleating towards either the inner or the outer side of the loop. These findings are in agreement with recent theoretical reports.

DOI: 10.1103/PhysRevB.64.104522 PACS number(s): 74.60.Ec, 74.25.Dw, 73.23.−b, 74.20.De

Ever since the original observation and explanation of flux quantization,[1,2] the superconducting flux quanta $\Phi_0 = h/2e$ have played a fundamental role in solid state physics. The concept of flux quantization has been crucial for the interpretation of a wide range of classical condensed matter experiments, concerning, e.g., weakly connected rings[3–5] and Little-Parks oscillations.[6–8]

However, all these investigations were primarily performed at temperatures close to the critical temperature T_c and at magnetic field intensities well below H_{c2}. Recently it has become possible with μ-Hall magnetometers to perform high-resolution magnetization experiments on small superconducting aluminum disks in the full magnetic field intensity range of superconductivity and at temperatures well below T_c.[9–11] These investigations have revealed information from deep within the superconducting phase, a regime that previously has not been accessible. Not unexpectedly these reports have attracted considerable interest also from a theoretical point of view.[12–20]

It is well known that for type-II ($\kappa = \lambda/\xi > 1/\sqrt{2}$) bulk superconductors a triangular Abrikosov vortex lattice is created in the magnetic field intensity range $H_{c1} < H < H_{c2}$, where κ is the Ginzburg-Landau parameter and H_{c1} and H_{c2} are the first and second critical fields. Since the effective Ginzburg-Landau parameter is significantly increased in thin films when the width of the film becomes comparable to the superconducting coherence length ξ_0, the appearance of an Abrikosov lattice is expected even in thin films consisting of type-I superconducting materials. When the spatial dimensions of the sample are decreased even further, and several length scales of the system become comparable with ξ_0, the competition between the Abrikosov vortex configuration and symmetry of the sample boundary becomes important. Hence for such mesoscopic systems the bulk critical fields H_{c1} and H_{c2} no longer are the only controlling parameters of the vortex configurations.

When considering sufficiently small superconducting rings the confinement effects from the boundaries are dominating and impose a circular symmetry on the superconducting order parameter. Hence the order parameter is expected to be given by $\psi(r) = F(r)e^{iL\theta}$, where L is the angular momentum or vorticity of the vortex. When the superconductor is described by such a circular symmetric order parameter it is said to be in a *giant vortex state*.[18–20] In a recent theoretical work the properties of giant vortex states and multivortex states in mesoscopic superconducting disks and rings were treated extensively.[24,25] It was found that the giant vortex state indeed is energetically favorable in narrow rings due to the strong influence of the ring surface. Furthermore, the superconducting state can consist of a combination of the paramagnetic and the diamagnetic Meissner state. In other words, the direction of the supercurrents closest to the outer edge are opposite to the currents running closest to the inner edge. This means that at a certain effective radius between the outer and inner edge, the supercurrent density goes to zero. Since this effective zero-current radius is the one that determines the area in which the flux is quantized, it becomes possible to measure this effective radius by studying the magnetization of superconducting mesoscopic loops. It was furthermore pointed out that when increasing the magnetic field intensity from zero field this effective radius would move towards the outer edge as a signature of the giant vortex state.

The measurement described in this paper was performed on a micron-sized superconducting aluminum loop placed on top of a μ-Hall magnetometer. The μ-Hall magnetometer was etched out of a GaAs/$Ga_{0.7}Al_{0.3}$As heterostructure. The mobility and electron density of the bare two-dimensional electron gas was $\mu = 42\ \mathrm{T}^{-1}$ and $n = 1.9\times 10^{15}\ \mathrm{m}^{-2}$. A symmetrical $4\ \mu\mathrm{m}\times 4\ \mu\mathrm{m}$ Hall geometry was defined by standard *e*-beam lithography on top of the heterostructure. In a later processing step a lift-off mask was defined on top of the μ-Hall probe by e-beam lithography. After deposition of a $t = 90$ nm thick layer of aluminum and lift-off the sample looked as presented in Fig. 1. The mean radius of the aluminum loop is $R = 2.16\ \mu$m and the average wire width w is 316 ± 40 nm. The superconducting coherence length was estimated to be approximately $\xi_0 = 180$ nm, corresponding to a bulk critical field of $H_{c2} = \Phi_0/2\pi\xi_0^2 \approx 100$ G.

By using the expression

$$n\Phi_0 = n\frac{h}{2e} = \Delta(\mu_0 H)\pi R^2, \tag{1}$$

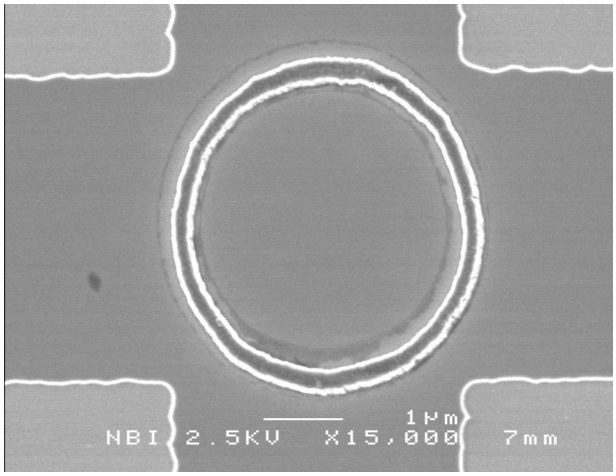

FIG. 1. Scanning electron microscope image of a μ-Hall probe; the cross section of the etched μ-Hall probe is 4×4 μm^2. The mean radius of the superconducting aluminum loop deposited on top of the μ-Hall magnetometer is 2.16 μm, and the difference between the outer and inner radius is 314 nm.

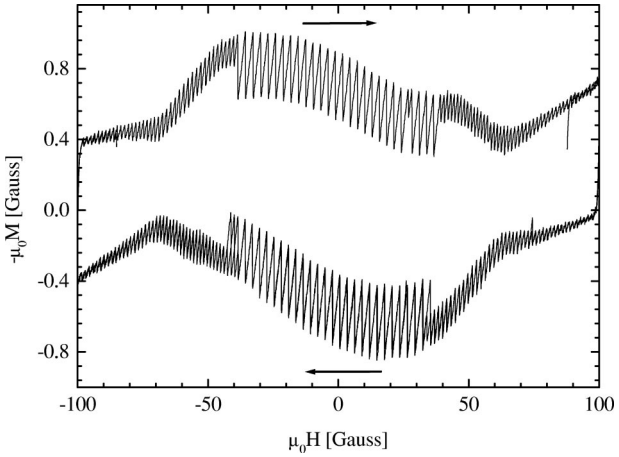

FIG. 2. Measured magnetization $\mu_0 M$ detected by the μ-Hall probe as a function of magnetic field intensity $\mu_0 H$ of the device presented on Fig. 1. The curve displays distinct jumps corresponding to the abrupt changes in magnetization of the superconducting loop when the system changes state. The measurements were performed at $T=0.36$ K.

where $A=\pi R^2$ is the area of the loop given by its mean radius R, it is found that a single flux jump ($n=1$) corresponds to a magnetic field periodicity given by $\Delta(\mu_0 H)=1.412$ G for the ring shown in Fig. 1.

The samples was cooled in a ^{3}He cryostat equipped with a superconducting solenoid driven by a dc current supply. The magnetic field intensity was changed in steps of 57.7 mG. Measurements discussed here were performed in the temperature range between $T=0.3$ K and the transition temperature of the superconducting loop $T_c\approx1.2$ K.

The relation between the Hall voltage V_H and the magnetic field intensity H perpendicular to the μ-Hall magnetometer is given by the classical Hall effect

$$V_H=-\frac{I}{ne}\mu_0(H+\alpha M), \tag{2}$$

where I is the dc current through the μ-Hall magnetometer and α is a dimensionless number of the order of unity, which corresponds to the ratio between the sensitive area of the μ-Hall probe and the area of the object that is the source of the magnetization M.[21,22] For our superconducting rings we find that α typically was in the range between 0.3 and 0.4.

By using standard ac lock-in techniques, where the driving current I was modulated, the Hall voltage V_H was measured as a function of magnetic field intensity $\mu_0 H$. Similar results to those presented here were observed in several samples with identical dimensions in a number of cooldowns. Also a circular loops with a width of $w=630$ nm, but with the same mean radius as the loops described above, were investigated.

In Fig. 2. is displayed the measured local magnetization $\mu_0 M$ detected by the μ-Hall probe as a function of magnetic field intensity $\mu_0 H$. The measurement was performed at $T=0.36$ K on the device presented in Fig. 1. The curve displays a series of distinct jumps corresponding to the abrupt changes in magnetization of the superconducting loop. The difference in magnetic field intensity between two successive flux jumps is approximately given by $\Delta(\mu_0 H)=1.4$ G or $\Delta(\mu_0 H)=2.8$ G, which corresponds to either single or double flux jumps ($n=1$ or $n=2$).

Large flux jumps ($n>1$) or flux avalanches occur whenever the system is trapped in a metastable state. It was generally observed that these flux avalanches become more pronounced with decreasing temperature, at low magnetic field intensities, and for wide loops. Furthermore, the flux avalanches were sensitive to the cooling procedure. The energy barrier causing the metastability of the eigenstates of the loop is due to either the Beam-Livingston surface barrier or the volume barrier, or even an interplay of both.[13,23,24]

In Fig. 3. the magnetic field intensity difference between successive jumps $\Delta(\mu_0 H)$, in units of the 1.412 G (corresponding to a single superconducting flux quantum), have been plotted as a function of magnetic field intensity. It is seen that the magnetic field intensity difference between the observed jumps is, to a high accuracy, given by integer values of 1.412 G. At absolute magnetic field intensities lower than 40 G double flux jumps dominate, whereas at higher absolute magnetic field intensities only single flux jumps are observed. The figure shows both an up-sweep and a down-sweep as indicated by the arrows.

Similar results obtained from the device with width $w=630$ nm are presented in Fig. 5. For these thicker loops it is seen that the flux avalanches are much more pronounced; avalanches corresponding to eleven single flux jumps were observed around zero magnetic field intensity. For these loops a gradual transition from huge flux avalanches ($n=11$) to single flux jumps occur as the magnetic field intensity is increased—similar to the sharp transition between double and single flux jumps observed for the thinner loops.

In the graphs presented in Fig. 3. it is seen that a small systematic variation of the value of the flux jumps occur when the magnetic field intensity is changed. This fine structure appears as a memory effect, in the sense that as the

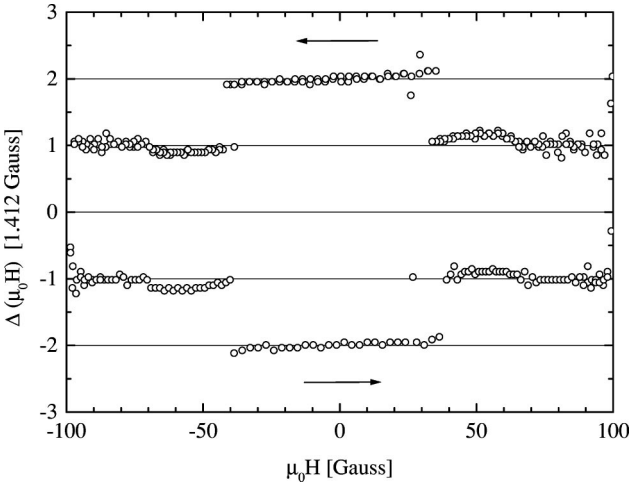

FIG. 3. The magnetic field intensity difference $\Delta(\mu_0 H)$ between two successive jumps in magnetization given in units of 1.412 G corresponding to a single flux quantum $\Phi_0 = h/2e$. The plotted jumps are given as a function of magnetic field intensity. The measurement was performed at $T = 0.36$ K. The positive (negative) flux values corresponds to the case where $\mu_0 H$ was decreased (increased) during the measurements. Arrows indicate sweep direction.

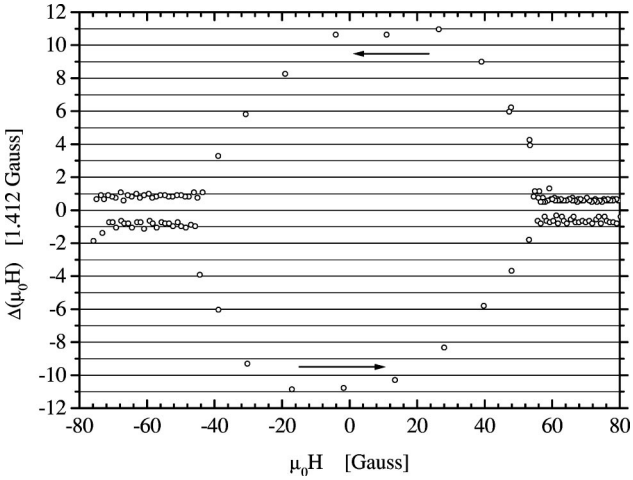

FIG. 5. The magnetic field intensity difference $\Delta(\mu_0 H)$ between two successive jumps in magnetization given in units of 1.412 G corresponding to a single flux quantum $\Phi_0 = h/2e$ for a loop with a width of $w = 630$ nm. The plotted jumps are given as a function of magnetic field intensity. The measurement was performed at $T = 0.38$ K. The positive (negative) flux values correspond to the case where $\mu_0 H$ was decreased (increased) during the measurements. Arrows indicate sweep direction.

magnetic field intensity is increased (decreased) the size of the flux jumps decreases (increases). Thus these deviations are dependent, not only on the size of the magnetic field intensity, but also on the direction the magnetic field intensity was swept through during measurements. The data presented in Fig. 3 have been replotted in Fig. 4 in the following way: We use Eq. (1) to calculate the effective radius R of the superconducting loop and plot this radius as a function of magnetic field intensity. The dotted horizontal lines in Fig. 4 represent the mean inner R_i and outer radius R_o determined from the scanning electron microscopy (SEM) picture. It is seen that as the magnetic field intensity is changed from negative to positive values, the effective radius, as defined from the flux quantization condition of the loop, changes from inner to outer radius and vice versa.

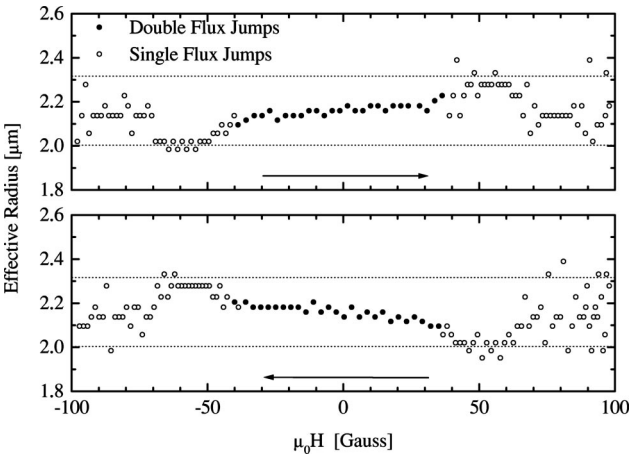

FIG. 4. Effective radius R calculated by using Eq. (1). The data points are the same as those presented in Fig. 3. Due to the fact that the measurements were performed by stepping the magnetic field intensity with a finite step, the effective radius is only measured with a precision of approximately 40 nm. The filled (open) dots corresponds to single flux jumps $n = 1$ (double flux jumps $n = 2$). The horizontal lines corresponds to the outer and inner radius determined from the SEM pictures. The arrows indicate sweep direction. It is seen that as the magnetic field intensity is changed, the effective radius changes between inner and outer radius of the loop, a change that depends on sweep direction and magnetic field intensity. The large spread of the data at high magnetic fields corresponds to regions where the amplitude of the oscillations measured by the Hall probe are small.

For a superconducting loop at low magnetic field intensities, it is expected that the appropriate effective radius is given by the geometrical mean value of the outer and inner radius $R = \sqrt{R_i R_o}$.[18,19,25] This is indeed in good agreement with the observed behavior around zero magnetic field intensity.

In the regime of high magnetic field intensities the concept of surface superconductivity becomes important and the giant vortex state will nucleate on the edges of the loop.[18–20] In this regime two degenerate current carrying situations are possible[26]—hence the giant vortex state can either circulate around the loop clockwise or anticlockwise.

Since the orientation of the current in the loop is determined by the sweep direction (Lenz's law), a decreasing (increasing) magnetic field intensity will give rise to a anticlockwise (clockwise) circulation. Hence as the magnetic field intensity is swept from, e.g., a large positive value to a large negative value the effective radius of the loop will change from inner to outer radius and vice versa, giving rise to the observed memory effect.

The width of the giant vortex state is approximately given by the magnetic length $l_H = \sqrt{\hbar/eH}$.[17] Hence any variation of the effective radius should take place over a magntic field

range given by the condition that the width of the loop and the magnetic length are comparable; $w = l_H$. Such an estimate gives a characteristic magnetic field intensity of 34 G in good agreement with the presented data in Fig. 4. A similar effective radius analysis of the data presented in Fig. 5 becomes rather dubious due to the combination of large flux avalanches and the larger width w.

At even larger magnetic field intensities ($|\mu_0 H| \approx 60$ G) the effective radius undergoes a transition from outer R_o (or inner radius R_i) to the mean radius R. We speculate that this could be due a two- to one-dimensional (2D-1D) transition due to an increase in the superconducting coherence length ξ_0 with magnetic field intensity.[20]

The characteristic dimensionless parameter used to distinguish between disks and loops is given by the ratio $x = R_i/R_o$ between outer and inner radius.[18–20] In our case the thin loops have $x = 0.86$, and for the thick loop to $x = 0.75$.

In recent work by two theoretical groups[18–20] it is found that at large x values (corresponding to a loop consisting of a one-dimensional wire) no or little variation of the effective radius should be observed, whereas at small x values (corresponding to a disk) a fast decrease of the effective radius occurs as the magnetic field intensity increases. In the intermediate regime $x = 0.5$, a rather smooth transition between the average and outer radius should take place when the magnetic field intensity increases.

In the presented measurement for the thinner loop ($x = 0.86$), we indeed observe that the effective radius varies smoothly between the inner and outer radius. This behavior looks similar to that predicted for loops with $x = 0.5$; however, it is not similar to that expected for $x = 0.75$. We do not find this discrepancy severe for the following reasons: The calculations by Bruyndoncx *et al.*[20] were done using the linearized first Ginzburg-Landau equation; hence these results are only valid close to the phase transition, viz., $R_o/\xi_0 < 1$. In the work by Peeters and co-workers[18,19] the full set of nonlinear Ginzburg-Landau equations were solved self-consistently, in the two cases where $R_o/\xi_0 = 4$ and 2. Neither of these conditions were fulfilled in our experiments, where we estimate $R_o/\xi_0 \approx 12$. It is furthermore seen by studying the results of Peeters *et al.* that calculations with larger values of R_o/ξ_0 probably would give rise to a better agreement.

For the thick loops ($x = 0.75$) we observed large flux avalanches at low magnetic field intensities. The large flux avalanches disguise any variation of the effective radius. Furthermore, the occurrence of flux avalanches in superconducting loops have not been dealt with quantitatively in the theoretical literature as far as the authors know. Hence comparisons with theory are not possible at the present time.

In summary, we present high-resolution magnetization measurements performed on superconducting aluminum loops. The resolution of the μ-Hall magnetometer allowed us to resolve subflux quantum effects and hence directly observe the dilation of a giant vortex state.

This work was financially supported by Velux Fonden, Ib Henriksen Foundation, Novo Nordisk Foundation, The Danish Research Council (Grant Nos. 9502937, 9601677, and 9800243) and the Danish Technical Research Council (Grant No. 9701490). The authors acknowledge Lars Melwyn Jensen, J. Berger, F. Peeters, and V.V. Moshchalkov for discussions.

*Present address: Department of Microelectronics and Nanoscience, Chalmers University of Technology, SE 412 96 Göteborg, Sweden.

[1] B. S. Deaver, Jr. and W. M. Fairbank, Phys. Rev. Lett. **7**, 43 (1961).
[2] R. Doll and M. Näbauer, Phys. Rev. Lett. **7**, 51 (1961).
[3] A. H. Silver and J. E. Zimmerman, Phys. Rev. **157**, 317 (1967).
[4] L. D. Jackel, W. W. Webb, J. E. Lukens, and S. S. Pei, Phys. Rev. B **9**, 115 (1974).
[5] L. D. Jackel, R. A. Buhrmann, and W. W. Webb, Phys. Rev. B **10**, 2782 (1974).
[6] W. A. Little and R. D. Parks, Phys. Rev. Lett. **9**, 9 (1962).
[7] R. D. Parks and W. A. Little, Phys. Rev. **133**, A97 (1964).
[8] R. P. Groff and R. D. Parks, Phys. Rev. **176**, 567 (1968).
[9] A. K. Geim, S. V. Dubonos, J. G. S. Lok, I. V. Grigorieva, J. C. Maan, L. T. Hansen, and P. E. Lindelof, Appl. Phys. Lett. **71**, 2379 (1997).
[10] A. K. Geim, I. V. Grigorieva, S. V. Dubonos, J. G. S. Lok, J. C. Maan, A. E. Filippov, and F. M. Peeters, Nature (London) **390**, 259 (1997).
[11] A. K. Geim, S. V. Dubonos, J. G. S. Lok, M. Henini, and J. C. Maan, Nature (London) **396**, 144 (1998).
[12] P. Singha Deo, V. A. Schweigert, F. M. Peeters, and A. K. Geim, Phys. Rev. Lett. **79**, 4653 (1997).
[13] P. Singha Deo, V. A. Schweigert, and F. M. Peeters, Phys. Rev. B **59**, 6039 (1999).
[14] V. A. Schweigert and F. M. Peeters, Phys. Rev. Lett. **81**, 2783 (1998).
[15] V. A. Schweigert and F. M. Peeters, Phys. Rev. B **57**, 13 817 (1998).
[16] J. J. Palacios, Phys. Rev. B **58**, R5948 (1998).
[17] R. Benoist and W. Zwerger, Z. Phys. B **103**, 377 (1997).
[18] F. M. Peeters, V. A. Schweigert, B. J. Baelus, and P. S. Deo, Physica C **332**, 255 (2000).
[19] B. J. Baelus, F. M. Peeters, and V. A. Schweigert, Phys. Rev. B **61**, 9734 (2000).
[20] V. Bruyndoncx, L. Van Look, M. Verschuere, and V. V. Moshchalkov, Phys. Rev. B **60**, 10 468 (1999).
[21] I. S. Ibrahim, V. A. Schweigert, and F. M. Peeters, Phys. Rev. B **57**, 15 416 (1998).
[22] F. M. Peeters and X. Q. Li, Appl. Phys. Lett. **72**, 572 (1998).
[23] C. P. Bean and J. D. Livingston, Phys. Rev. Lett. **12**, 14 (1964).
[24] X. Zhang and J. C. Price, Phys. Rev. B **55**, 3128 (1997).
[25] R. M. Arutunian and G. F. Zharkov, J. Low Temp. Phys. **52**, 409 (1983).
[26] See, e.g., M. Tinkham, *Introduction to Superconductivity*, 2nd ed. (McGraw-Hill, New York, 1996), pp. 141–143.